

# Multilayer coatings for femto- and attosecond technology

O. RAZSKAZOVSKAYA,<sup>1</sup> F. KRAUSZ,<sup>1,2</sup> AND V. PERVAK<sup>2,3,\*</sup>

<sup>1</sup>Max-Planck Institute of Quantum Optics, Hans-Kopfermann-Str. 1, D-85748 Garching, Germany

<sup>2</sup>Ludwig-Maximilian Universität München, Am Coulombwall 1, D-85748 Garching, Germany

<sup>3</sup>Ultrafast Innovations GmbH, Am Coulombwall 1, D-85748 Garching, Germany

\*Corresponding author: vladimir.pervak@physik.uni-muenchen.de

Received 5 October 2016; revised 20 December 2016; accepted 20 December 2016 (Doc. ID 278214); published 12 January 2017

Chirped multilayer mirrors have permitted mode-locked lasers to routinely generate pulses in the sub-10 fs regime. Continuous progress in the design, manufacturing, and characterization of multilayer structures has led to ever more precise group-delay dispersion control over ever broader spectral ranges. The resultant few-cycle laser fields have opened the door to the generation and measurement of isolated attosecond pulses and led to the birth of attosecond metrology. Precision multilayer dispersion control over increasing bandwidth has gradually pushed the frontier of femtosecond technology to what has been thought to be its ultimate limit: the wave cycle of visible light, allowing routine generation of sub-100 attosecond pulses. Next-generation attosecond technology will be based on synthesized multi-octave waveforms; they are expected to advance the field in several ways: first, by permitting control of electronic motions with a force variable on the atomic time scale; second, by providing sub-femtosecond optical transients for attosecond nonlinear pump-probe spectroscopy; third, by producing attosecond pulses at Angstrom wavelengths, opening the door to four-dimensional imaging with atomic resolution in space and time. In this article, we address the enabling technology: chirped multilayers for spectral separation and recombination as well as precise dispersion control of multi-octave optical radiation spanning from the ultraviolet to the mid-infrared range. This cutting-edge optical technology provides the force engineerable on atomic-to-molecular time scales and brings about the next revolution in ultrafast science. © 2017 Optical Society of America

**OCIS codes:** (310.4165) Multilayer design; (310.6845) Thin film devices and applications; (320.5520) Pulse compression; (320.1590) Chirping.

<https://doi.org/10.1364/OPTICA.4.000129>

## 1. INTRODUCTION

Observing and controlling fast-evolving processes relies on light flashes with a duration substantially shorter than the time evolution of the process of interest. The quest for ever-shorter pulses started shortly after the first laser was demonstrated [1] and rapidly led to sub-100 fs pulses by passively mode-locked dye lasers [2–6].

After a reign of two decades, femtosecond dye lasers were replaced by Kerr-lens mode-locked Ti:sapphire lasers, in which self-phase modulation and group-delay dispersion (GDD) control by a pair of prisms allowed the pulse duration to approach [7,8] and surpass the 10 fs regime for the first time [9]. Uncompensated higher-order dispersion was found to be the limiting factor in further pulse shortening [9,10], while the delicacy of the prism arrangement challenged the reproducible operation. Replacing the prisms with aperiodic multilayer resonator mirrors with tailored GDD [11], which became known as chirped mirrors, allowed these limitations to be overcome. With their use, Stingl *et al.* [12,13] demonstrated the generation of highly stable sub-10 fs optical pulses from a Kerr-lens mode-locked Ti:sapphire

laser. Over the next decade, the capability of chirped mirrors to reflect light over a broad range of wavelengths with controlled phase, combined with simplicity and high efficiency, had been instrumental in advancing Ti:sapphire oscillators to the few-femtosecond, few-cycle regime [14–19].

Discovery of nonlinear pulse compression [20–24] slowly pushed the achievable spectral bandwidths to an optical octave. Precise and versatile techniques for manipulation of the temporal profile of ultrashort pulses were in demand. Programmable pulse shapers [25] got into the spotlight. They include liquid crystal arrays [26,27], deformable mirrors [28], and acousto-optic programmable dispersive filters (AOPDFs) [29,30]. Programmable pulse shapers provide unprecedented flexibility for amplitude and phase shaping of the spectra, along with the possibility of on-demand tuning. However, they come at the expense of non-negligible disadvantages. Liquid crystal arrays and deformable mirrors need to be placed in the Fourier plane of a 4-f system, thus often becoming a cumbersome arrangement. In addition, their efficiency is limited by the efficiency of involved diffraction gratings. Deformable mirrors are also constrained by the

maximum amplitude of the deformation. AOPDF has rather low efficiency while operating on the broadband spectra. As a result, despite their lack of flexibility, dispersive multilayer mirrors retained their leading positions in the field of dispersion control over broadband spectra.

By the turn of the millennium, nonlinear pulse compression of amplified pulses along with the progress of dispersive mirror technology [31] extended the frontiers of ultrashort pulse generation to what has been believed to be an ultimate border—one cycle of the optical carrier wave. Advanced chirped-mirror-based ultrafast systems nowadays routinely deliver powerful near-single-cycle pulses [32,33], which in turn enable the generation of trains of and isolated attosecond extreme ultraviolet pulses [34–36].

To this end and more generally for the control of electronic phenomena with the electric force of light, precise control and shaping of the electric field evolution (henceforth “optical field”) is of crucial importance [37,38]. Shifting the phase of the carrier wave with respect to the pulse envelope, referred to as the carrier-envelope phase (CEP), constitutes the simplest means of modifying the temporal evolution of the optical field. This modification preserves the sinusoidal field evolution and introduces a sub-cycle change in the amplitude evolution for pulse duration comparable to the carrier wave cycle.

More versatile control of atomic-scale electronic motion requires sculpting of the field evolution on an attosecond time scale, i.e., *within the wave cycle of light*. This calls for super-octave bandwidth and control schemes more sophisticated than simple adjustment of the CEP. Sub-cycle tailoring of optical fields can be implemented by changing the relative time delays between several coherently recombined CEP-stable wavepackets carried at different wavelengths. This generic approach constitutes the basis of optical waveform synthesis (OWS). The first successful implementations of the OWS concept were based on stimulated Raman scattering [39], the synchronization of independent ultrafast sources [40], or fiber amplifiers jointly seeded with a spectral continuum [41].

More recently, multi-octave, phase-stable supercontinua produced by self-phase modulation of sub-millijoule femtosecond pulses in gas-filled hollow fibers have been spectrally subdivided and, after precision GDD and CEP control as well as delay of the separated wavepackets, coherently recombined. The approach has yielded optical field transients with non-sinusoidal waveforms [42], including some with durations shorter than 1 fs [43]. The output energy of this “passive” non-amplifying (henceforth “passive”) scheme is limited to a fraction of the energy of the seed continuum, typically in the multi-microjoule to sub-millijoule regime. This passive scheme can be turned into an active one by incorporating optical parametric amplifiers (OPAs) in the individual spectral channels. In this case, the synthesizer can then be seeded at lower energy, which is then boosted by many orders of magnitude in broadband OPA stages [44–48]. Such an OPA-based, “active” optical waveform synthesizer (henceforth “active”) holds promise for delivering multi-octave transients with multi-millijoule energy and multi-TW peak power.

Both the passive and active schemes are similar in that they rely on chirped mirrors. Following the demands of the OWS, chirped mirror technology had to be extended from the visible (VIS) and near-infrared (NIR) range around the spectrum of Ti:sapphire toward the ultra violet (UV) and the infrared (IR), where chirped mirrors have been hardly available [49]. In this work, we discuss

the specific demands on the optics required for OWS, challenges associated with the different spectral domains spreading over several octaves, and design approaches that address these challenges, and we demonstrate the most recent progress in the field of dispersive optics for OWS.

We start by addressing the problem of dividing multi-octave radiation into different spectral channels while preserving the spectral phase and amplitude distribution of the light wave, and then move on to discuss the broadband dispersive multilayer mirrors required for GDD control over the individual spectral ranges. We give an overview of multilayer optics for the VIS and NIR range of Ti:sapphire lasers and then address the latest advances that extend precision GDD control into the UV and toward the mid IR.

## 2. MULTI-OCTAVE GROUP DELAY CONTROL

Independent of the specific scheme, OWS relies on seed pulses with ultra-broad spectral coverage, spanning preferably a couple of octaves or more. The spectrum is separated into several channels, of which each is treated individually. In the case of the passive scheme, each channel is compressed to near its Fourier-transform-limit (FTL) in a dispersive delay line, before being recombined to synthesize the transients. In active schemes, each wavepacket remains temporally stretched while being amplified in one or more OPA stages. In [50], Chia and co-workers suggested keeping the individual channels slightly chirped until after the final recombination in order to decrease the peak intensity and thus reduce the B-integral. The ultra-broadband dispersive mirror pair was meant to compensate the dispersion of the combined waveform afterward. The laser-induced damage threshold of the final mirror pair still remains a concern.

The channels of any OWS apparatus are initially separated with customized dichroic beam splitters (DBS). There are several major requirements to these key components: (1) a high contrast between reflected and transmitted light; (2) a “cross-talk” region between channels that is used for channel-to-channel synchronization; and (3) smooth, well controlled (preferably flat) phase of *both* reflected *and* transmitted spectra in order to ensure compressibility of the individual channels. Fulfillment of all three requirements simultaneously is a formidable task [50]. Conventional DBSs are based on quarter-wave stacks of alternating high- and low-refractive-index dielectric layers. Their high-reflectance (HR) band is determined by the contrast between the refractive indices of the coating materials and is typically much narrower than the desired spectral span of the individual synthesizer channel. While exhibiting negligible GDD within the central region of their HR band, they are plagued by strong group delay (GD)/GDD ripples at the edges of the zone, which is intolerable in applications for OWS. In order to extend the HR zone to the desired bandwidth and suppress dispersion ripples in the transition zones, the layer thicknesses are numerically optimized. The resultant slight detuning from a quarter-wave structure also creates the required “cross-talk” zones.

Beyond the just-mentioned criteria, the DBSs of the OWS have to fulfill general requirements for mirrors used in demanding applications, such as compensation for the tensile stress caused by the multilayer coating itself. In the case of an interferometric setup such as an OWS, this is particularly important in order to match the wavefronts of the individual channels and ensure their optimal superposition across the entire beam. This critical

requirement is met by applying a compensatory coating on the back surface of the mirror substrate.

The designed reflectance and GD for the class of DBSs used for separating the UV, VIS-UV, and VIS channels in OWS in [43] and VIS and NIR from IR in an OPA-based active OWS under development are presented in Fig. 1. The DBSs characterized by the curves in the Fig. 1 well fulfill the above-mentioned major requirements demanded by OWS applications: (1) there is a high contrast between high-reflectance and high-transmittance zones, yet (2) there are relatively narrow transition zones between the channels and (3) the GD is smooth for both the high-reflectance and high-transmittance zones, even including the transition regions. These DBSs can be used for splitting as well as for recombining the beams.

### 3. VISIBLE DISPERSIVE OPTICS

Broadband dispersive multilayer mirrors in the VIS and NIR have matured over the decades. In their first applications, dispersive mirrors aimed to introduce constant negative GDD over a selected spectral range [51,52]. Several design approaches have been applied to improve mirror performance [53,54].

In the pursuit of near-single-cycle light, the required working bandwidth rapidly approached an optical octave [21,55]. Under

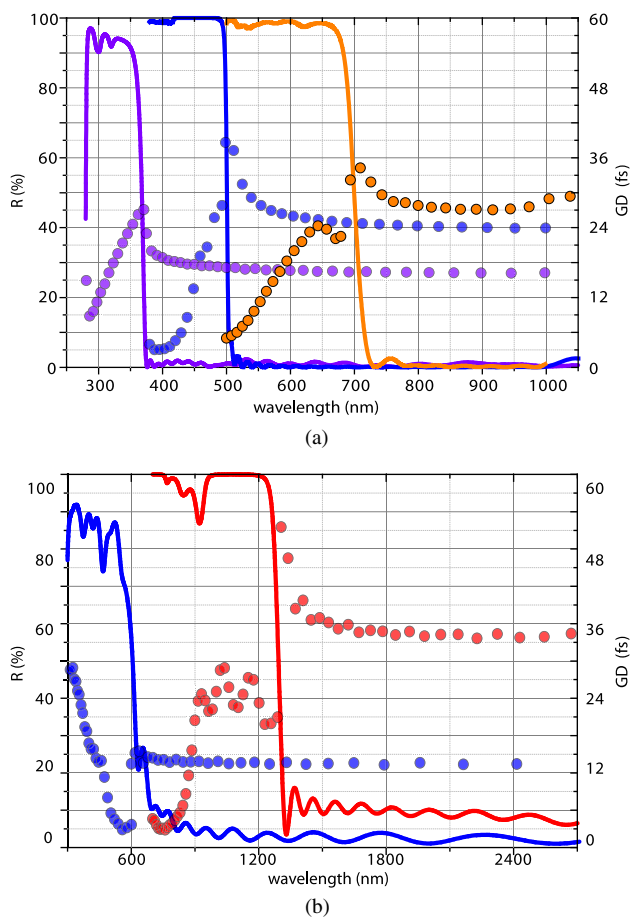


**Fig. 1.** Dichroic beam splitters for optical waveform synthesis. (a) Class of dichroic beam splitters for separation of ultraviolet, visible, and near-infrared bands in the passive synthesizer in [43]. (b) Class of dichroic beam splitters for separation of visible and near-infrared bands in the passive and active synthesizers under development. Solid curves, designed reflectance; dotted curves, designed GD.

these conditions, control of GDD to the lowest order became insufficient for achieving transform-limited pulses and more sophisticated designs were needed. Double-chirped mirrors [56–58], complementary mirror pairs [59], and double-angle mirrors [60] enabled significant extension of the bandwidth and simultaneous control over the higher-order dispersion. Evolution of the design tools and computational power has also been instrumental in the progress of the thin-film multilayer coatings for ultrafast optics [61–63].

As a result, the state-of-the-art chirped mirrors nowadays are able to operate over super-octave spectra and compensate the phase to an arbitrary dispersion order [50,64]. However, the accurate initial definition of the dispersion target remains a major challenge for the development of broadband dispersive multilayers.

#### A. Phase Compensation Versus Material Compensation

The main goal of the dispersion management in the case of pulse compression is to compensate for spectral phase variations; therefore, the precise control of it is of utmost importance. A major prerequisite is accurate knowledge of the spectral phase to be compensated for. Several techniques have been developed for measuring this quantity, allowing (together with the spectral amplitude) complete characterization of the ultra-short laser pulses [65–67]. Unfortunately, most of the techniques are not without shortcomings. These include the presence of ambiguities, insufficient temporal and/or spectral resolution and/or range, inherent inability to measure the complete pulse intensity and/or phase, inability to measure complex pulses, and artifacts due to multi-shot averaging over pulses with fluctuating characteristics [68]. As a result, the phase retrievals may be inconsistent and/or inaccurate, and thus compromise the accuracy of the target for dispersive multilayer development (henceforth “dispersion target”).

Whenever the chirp carried by the laser pulse to be compressed is dominated by material dispersion, it may be more reliable to aim at canceling this material dispersion, which is well known. Therefore, in the material compensation approach, the dispersion target is chosen to compensate for the dispersion accumulated by the initially compressed pulse after propagation through known materials (including air). Since the optical constants of the commonly used optical materials and gases are well known, the resulting target can be calculated with a high accuracy, with the only remaining source of uncertainty being nonlinear effects.

Figure 2 presents two group delay versus wavelength dispersion targets for mirrors to be used in the VIS spectral range. The material-based dispersion target (blue curve) in Fig. 2 was designed to compensate for dispersion introduced by 2 mm of fused silica and 1 m of air with four bounces on double-angle dispersive mirrors. The phase-based target (red curve) was derived from a measured spectral phase. While the material-based target is clearly dominated by the second- and third-order dispersion, the phase-based target is noticeably influenced by the higher orders. These higher orders are likely inherited from the paternal nonlinear process (for example, broadening in a hollow-core fiber) or accumulated upon propagation due to induced nonlinearities.

In rare cases, when the accurate measurement of the spectral phase is hindered and compensation for material dispersion only does not yield the desired quality of compression, a hybrid approach may be helpful. In this case, the initial target is approximated by the known material dispersion. With the first set of

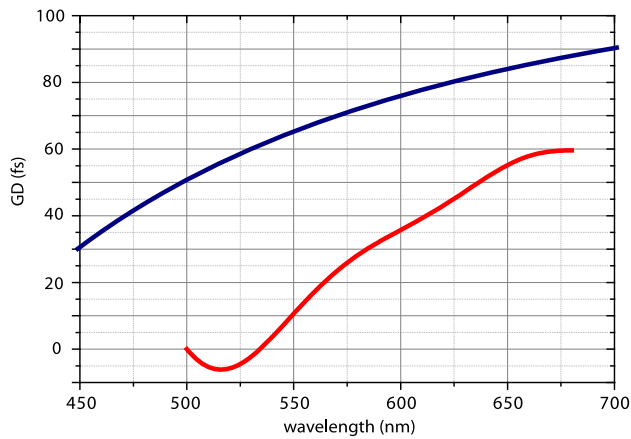
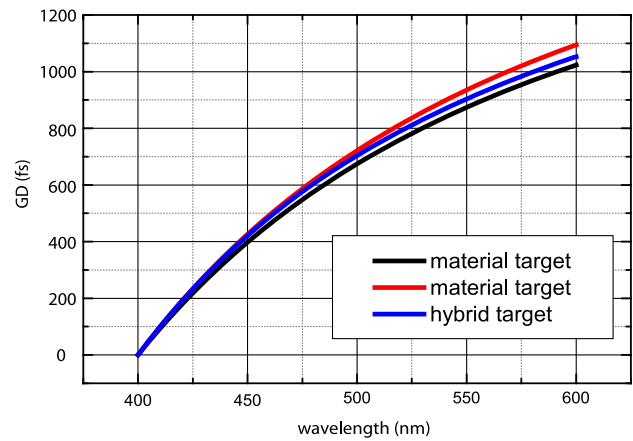


**Fig. 2.** Dispersion targets developed based on the phase compensation (red curve) and material compensation (dark blue curve) approach. The vertical offset is introduced for illustration purposes.

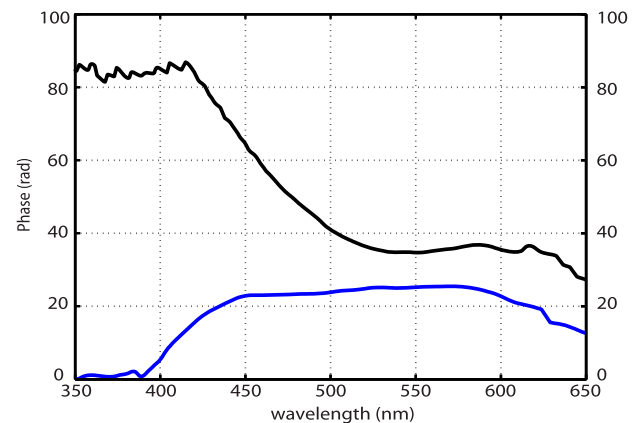
dispersive optics produced in this way, the residual phase is either carefully measured or compensated for by a programmable dispersive filter [29,30]. The new target is corrected for this residual phase. A dispersion target developed following the hybrid approach is presented in Fig. 3. The black curve in Fig. 3(a) is the initial dispersion target calculated to compensate for a particular amount of material dispersion in the optical system. After the first optics were produced and implemented, it was found that the blue edge of the spectrum (wavelength range 400 to 450 nm) required additional dispersion [red curve in Fig. 3(a)]. The new hybrid dispersion target was then designed to introduce the missing residual dispersion identified in the just-mentioned procedure (blue curve). The reconstructed spectral phases of the ultrashort pulses achieved with material-only and hybrid approaches are presented in Fig. 3(b). The spectral phase of the 6.1 fs pulse achieved via hybrid compression (blue curve) is noticeably flatter in the working spectral range than the spectral phase of the 15 fs pulse achieved with material compensation only, thus obviously yielding the better compression. The hybrid approach is powerful at the expense of increased time and material consumption.

The production of multiple layers that precisely reproduce the dispersion target over the entire bandwidth is challenging. Dispersive multilayer coatings are very sensitive to deposition errors, as even slight changes in the layer thicknesses affect the spectral phase, so high-precision deposition techniques are required to ensure reliable production. Magnetron and ion beam sputtering are well-established processes for the production of dielectric multilayer optics for the VIS and NIR spectral ranges that offer higher accuracy and reproducibility than electron beam evaporation. Consequently, the coating materials are often chosen to be compatible with either of the methods.

The working spectral range of a thin-film coating is defined by the transparency regions of the coating materials. A pair of layer materials with large contrast between their refractive indices is highly beneficial for broadband control of optical radiation. Currently,  $\text{Ta}_2\text{O}_5/\text{SiO}_2$  and  $\text{Nb}_2\text{O}_5/\text{SiO}_2$  are the two most commonly used material pairs for production of the dielectric thin-film coatings for the VIS and NIR spectral ranges. Their low absorptance and high refractive index contrast (2.12/1.47 for  $\text{Ta}_2\text{O}_5/\text{SiO}_2$  and 2.28/1.47 for  $\text{Nb}_2\text{O}_5/\text{SiO}_2$  at 800 nm



(a)



(b)

**Fig. 3.** Hybrid dispersion target approach for the design of the visible and near-infrared dispersive mirrors. (a) Hybrid dispersion target for the design of visible and near-infrared dispersive mirrors. (b) Pulse compression with hybrid target. Black curve shows spectral phase of the 15 fs pulse achieved with material compensation only. Blue curve shows spectral phase of the 6.1 fs pulse (FTL = 6 fs) achieved with hybrid compensation.

[69]) permit the production of multilayer structures with high reflectance and low loss in the VIS spectral range.

The multilayer mirrors following the dispersion targets in Fig. 2 were produced by magnetron sputtering deposition process. The agreement between designed and measured characteristics demonstrates the reliability of the technology (Fig. 4). Upon implementation, both designs yielded well-compressed, nearly transform-limited pulses: 6.5 fs (6.1 fs FTL) [Fig. 4(a)] in the case of phase-based target and 2.9 fs (2.7 fs FTL) [Fig. 4(b)] in the case of the material-based target, therefore validating the suitability of both approaches.

Overall, significant developments in the field of dispersive coatings stimulated by the demands of the ultrafast optics allow for a versatile and reliable dispersion management in the VIS and NIR spectral ranges.

#### 4. ULTRAVIOLET DISPERSIVE OPTICS

For almost two decades after the first demonstration of dispersive multilayer mirrors [11], their evolution responded to the demands of Ti:sapphire-based systems, with little effort being

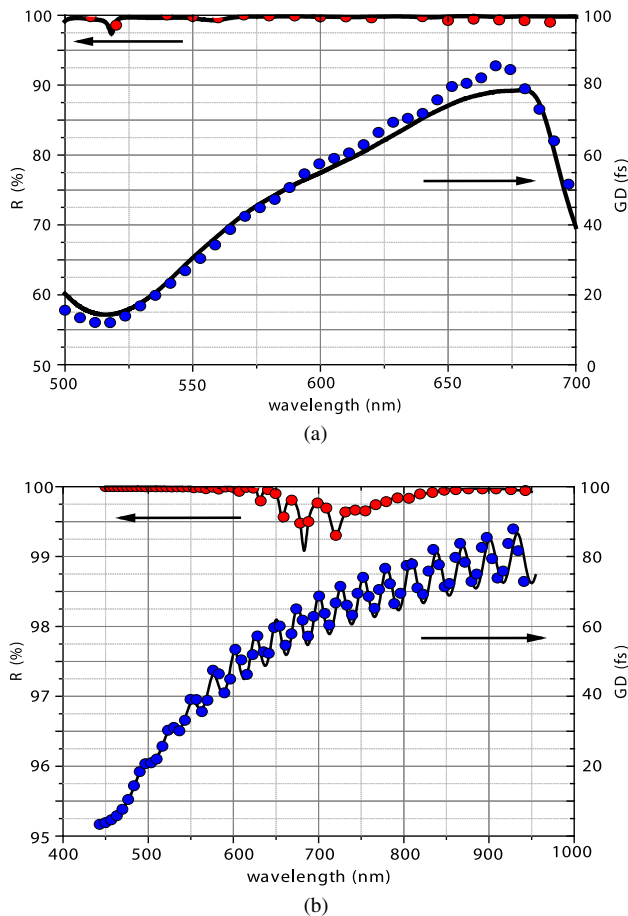


**Fig. 4.** Dispersive multilayers in visible spectral range. (a) Dispersive multilayer developed upon phase compensation dispersion target. (b) Dispersive multilayer developed upon material compensation dispersion target. Black solid curves, designed reflectance/GD; dotted red curve, measured reflectance; dotted blue curve, measured GD.

invested into the extension of the technology into the UV spectral range [70]. Generation of the synthesizer's spectrum via broadening of the femtosecond Ti:sapphire pulses in a gas-filled hollow-core fiber [42,43] gives rise to a significant extension of the spectral range into the UV. Consequently, it is possible—and for many applications desirable—to extend the synthesizer's spectral coverage to the UV spectral range.

UV is a notoriously difficult working range in terms of dispersion control for broadband radiation, because the refractive index and absorption rapidly increase as the frequency of the incident radiation approaches atomic resonances in the UV, resulting in strong dispersion and often non-negligible absorption over even relatively short propagation distances.

Manufacturing of precision dispersive multilayers in the UV is significantly more challenging. The physical thickness of the individual layers scales with the central wavelength, and thus it becomes smaller for shorter wavelengths, while the absolute deposition error remains approximately unchanged. Consequently, the relative error in layer deposition tends to be higher in the UV than in the VIS-IR range. As a result, electron-beam evaporation of the  $\text{HfO}_2/\text{SiO}_2$  material pair, the well-established standard technology for the production of high-reflectivity mirrors and filters in the UV, is unsuitable for the manufacturing of

dispersive optics for UV. The accuracy of this deposition technique entails intolerable errors for chirped multilayers in the UV. Fortunately, the deposition of this material pair has recently been adapted for magnetron sputtering [71] and ion-beam sputtering, enabling the deposition of layers with higher accuracy. This progress has been instrumental in extending broadband dispersive multilayers into the UV range. Another major challenge has turned out to be the optical properties of the thin-film materials themselves.

### A. Induced Nonlinear Effects

While progress in ultra-short pulse generation, assisted by dispersive multilayers, has been beneficial for advances in the field of nonlinear optics, modeling of thin-film multilayer coatings has so far excluded nonlinear effects. Their reflectance, transmittance, and dispersion were evaluated on the basis of the linear optical properties of the layer materials. Our recent work has demonstrated that this approach may be inappropriate while working in the UV.

The dispersive multilayer mirrors employed in strong field experiments are typically exposed to intensities on the order of  $10^{10}$  W/cm<sup>2</sup> to  $10^{12}$  W/cm<sup>2</sup>. This regime is dominated by the bound electronic nonlinearities related to the second- and third-order electric susceptibility. The appearance of these nonlinearities in bulk media is known and taken into account upon designing of the apparatus. However, as the average thickness of the thin-film multilayer for the visible spectral range is about 7  $\mu\text{m}$  and nonlinear refractive indices of the most commonly used coating materials are rather small in this range, it was assumed and accepted that thin-film coatings are not susceptible to nonlinearities until intensities reaching nearly the laser-induced damage threshold.

In our recent work, we uncovered the fact that dispersive multilayer structures might be affected by a nonlinear polarization response for incident intensities significantly lower than the damage threshold due to strong local field enhancement. In the UV range, when nonlinear refraction and two-photon absorption rapidly increases [72], this enhancement becomes sufficient to trigger the appearance of the third-order nonlinearities that are otherwise not observed [73]. However, the effect is not only bound to the UV [74]. Therefore, the optics of the future high-energy active OWS systems might be affected and these effects should be taken into account.

### B. Establishing Control Over Induced Nonlinearities

To prevent small nonlinearities from adversely affecting the dispersive properties of chirped multilayers, it is desirable to take the nonlinear absorptance and the nonlinear refractive index into account. In the absence of reliable experimental data on nonlinear refractive indices and two-photon absorption coefficients of commonly used dielectric coating materials over the broad spectral ranges of interest, accurate incorporation of these parameters into the design routine is unfortunately not possible. At the present, only approximate modeling based on estimated values of nonlinear coefficients is feasible.

In our recent work [73], we have found a way to estimate the two-photon absorption coefficient for a spectral range of interest from the experimental data and to incorporate it into the design procedure. We showed that undesirable nonlinear absorptance can be efficiently suppressed by substituting a significant amount

of the high-index-layer material with low-index-layer material. As the two-photon absorption coefficients are inversely proportional to the electronic band gap of the materials [72], the low-index materials have much weaker induced absorptance and therefore their properties are much less intensity dependent.

We have recently implemented this approach in the design of a UV dispersive multilayer for a passive OWS [43], using an “effective” spectrally averaged two-photon absorption coefficient estimated from the experiment [75]. Figure 5 illustrates the key points of the approach. It shows designed reflectance of the optimized and non-optimized UV dispersive multilayer. The gray curve shows the reflectance of the non-optimized design without any of the nonlinear absorptance taken into account, the blue curve shows the reflectance of the non-optimized design affected by the nonlinear absorptance, and the red curve shows the reflectance of the optimized design with nonlinear absorptance taken into account. There is a clear improvement of averaged reflectance from the non-optimized to optimized design. The improvement is reached by modification of the initial, non-optimized design depicted in the Fig. 5(b), with a significant amount of high-index material being substituted by low-index material. The resultant multilayer stack of the optimized design is presented in Fig. 5(c).

The optimization for minimum two-photon-induced absorptance has to preserve the dispersion properties of the mirror [Fig. 5(a)]. This was achieved by suitable adjustment of the low-index replacement layers to ensure the required optical delay. Consequently, the replacement layers need to be thicker, yielding an increased physical thickness of the overall coating. This, in turn, increases the risk for excessive tensile stress.

Modification of the stack alternates the distribution of the electric field in the multilayer coating (Fig. 6). The enhancement is reduced and the peaks of the electric field are re-situated in low-index layers. As the distribution of the electric field is also known to strongly influence the damage thresholds of the thin-film coatings [76,77], the modified distribution yields a potentially higher damage threshold.

Extending dispersive mirror technology further into the UV calls for exploration of new materials. One of the prospective alternatives is the  $\text{Al}_2\text{O}_3/\text{SiO}_2$  pair. However, the much lower refractive index contrast (1.84/1.50 versus 2.25/1.50 for  $\text{HfO}_2/\text{SiO}_2$  at 250 nm [69]) will require more layers and overall thicker coatings to be deposited in order to achieve a similar introduced GD. At the same time, the high precision of the deposition process needs to be maintained. The fulfillment of the both criteria is possible by transferring the technology to ion-beam sputtering deposition plants.

## 5. INFRARED DISPERSIVE OPTICS

There are a number of reasons for extending the capability of optical waveform synthesis into the IR spectral range; they include the exploration of strong-field phenomena in solids [78] and the generation of isolated attosecond x-ray pulses via extending high-harmonic generation into keV photon energies [79–81]. These prospects sparked interest in the development of ultrafast sources with spectral coverage extending into the mid IR [82–84], including schemes for OWS [46,48].

Just as in the UV, the development of dispersive optics for IR lags behind, but for a different reason: the lack of scientific interest. Starting from the wavelength of 1.5  $\mu\text{m}$ , most of the

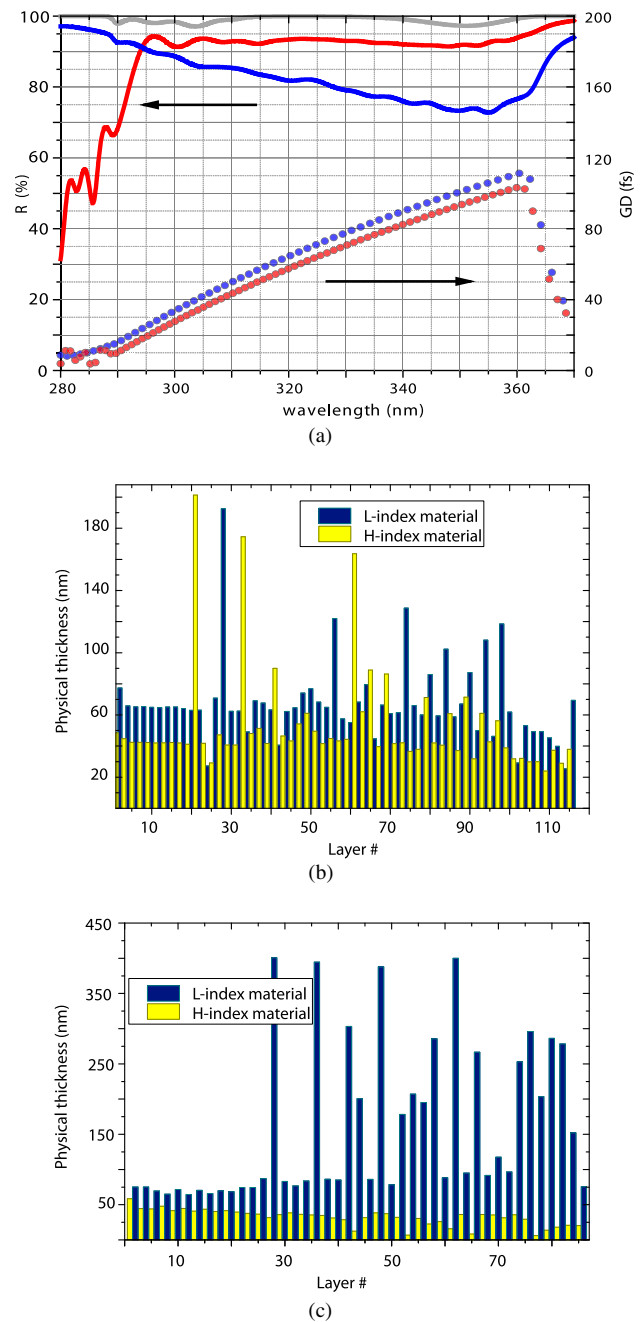


**Fig. 5.** Gaining control over induced nonlinear effects. (a) Solid curves, designed reflectance of the non-optimized multilayer mirror without (gray) and with (blue) nonlinear absorptance taken into account, and of the optimized design with nonlinear absorptance taken into account (red). Working intensity is  $0.25 \times 10^{10} \text{ W/cm}^2$ . Dotted curves, designed GD of the optimized (red) and non-optimized (blue) mirrors. Vertical offset of the GD curves is for illustration purposes. (b) Layer sequence of the non-optimized mirror. (c) Layer sequence of the optimized mirror. Figures (b), (c), and partially (a) reproduced from [75].

commonly used optical materials change from positive to negative group-velocity dispersion (GVD), while Si and Ge maintain positive GVD through the mid-IR range. Consequently, it becomes possible to perform compression in bulk by carefully balancing the materials with opposite GVD in the beam path [83,85,86]. Unfortunately, the approach works well only for dispersion compensation to lowest-order (GDD), with high-order

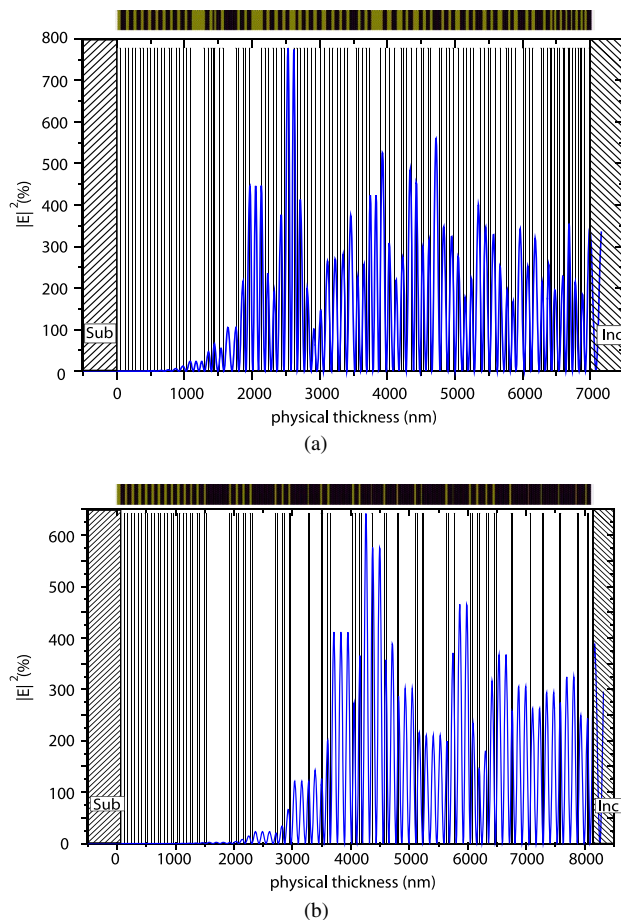


**Fig. 6.** Gaining control over induced nonlinear effects: distribution of the electric field inside the multilayer structures. (a) Electric field distribution inside the non-optimized dispersive multilayer stack. (b) Electric field distribution inside the optimized dispersive multilayer stack. Dark yellow bands, high-index material; brown bands, low-index material.

contributions to dispersion, which are essential for few-cycle pulses, left uncompensated [85]. In addition, with its band gap of 1.11 eV (at 300 K), Si is susceptible to two-photon absorption, restricting the maximum incident intensity. Implementation of dispersive multilayer mirrors offers an elegant solution for circumventing these shortcomings.

Two alternative chirped mirror designs covering the IR range spanning from 1.6 to 2.7  $\mu\text{m}$  are presented in Fig. 7. The design illustrated in Fig. 7(a) imitates dispersion introduced by 0.25 mm of Si; the design in Fig. 7(b) follows an alternative target. While it introduces the GDD equivalent of 0.25 mm Si at the central wavelength, the sign of the third-order dispersion is changed to negative.

As the thickness of the individual layer of the multilayer design scales with the central wavelength of the incident spectrum, multilayer structures in the IR tend to be substantially thicker than their counterparts designed for VIS or UV wavelengths. For example, the physical thickness of the coatings in Fig. 7 approaches 20  $\mu\text{m}$ . The risk of excessive tensile stress, which might affect the mechanical properties of the deposited structure and make it peel off from the substrate, increases. The overall physical thickness must therefore be traded off against bandwidth, dispersion, and reflectance of the dispersive mirror, all of which tend to

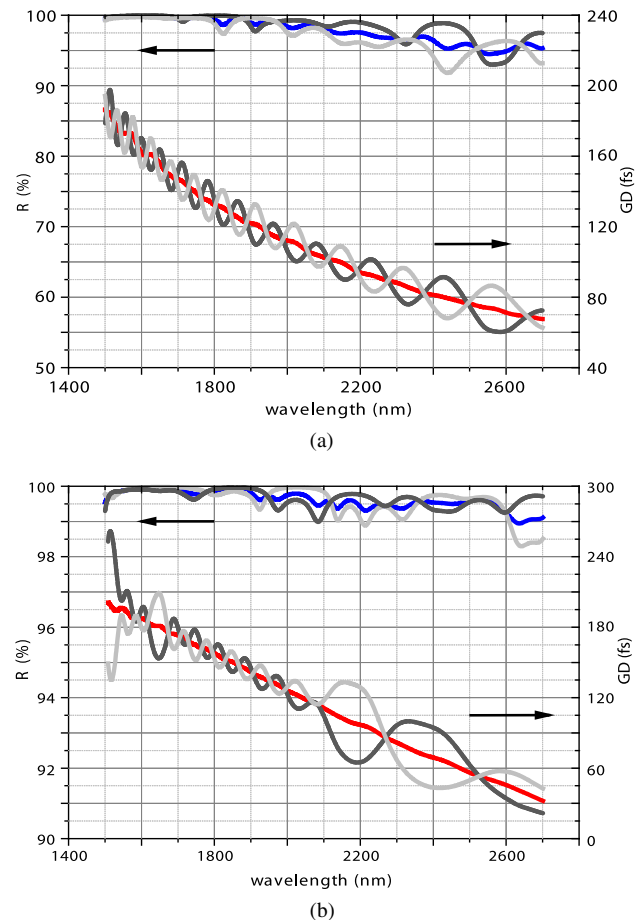


**Fig. 7.** Dispersive multilayers in the infrared spectral range designed to compensate the material dispersion of 0.25 mm Si to the lowest order. (a) Dispersion target and design imitating 0.25 mm Si. (b) Dispersion target and design introducing second-order identical to 0.25 mm Si, yet with negative third-order dispersion. Gray, dark gray curves, the designed GD curves of an individual mirror of the mirror pair; red curve, resulting designed averaged GD; gray, dark gray curves, reflectance of the individual mirror of the mirror pair; blue curve, resulting averaged reflectance.

increase with increasing number of layers and hence structure thickness. For instance, the design in Fig. 7(b) was allowed to be slightly thicker and contain more layers than the design in Fig. 7(a), resulting in higher reflectance and improved pulse-compression efficiency.

Fortunately, the limitation to the maximum physical thickness is not a fundamental one. The mechanical stress may be reduced by tuning the parameters of the deposition process at the expense of changes in the optical properties of the layers. These changes must be well understood and controlled before the approach can be used for the production of thicker structures.

Unlike in the UV, there are several layer materials excellently suited for multilayer development in the IR range. The already-mentioned material pair exploited in VIS/NIR,  $\text{Nb}_2\text{O}_5/\text{SiO}_2$ , is transparent until 8  $\mu\text{m}$ . For the spectral region beyond 2  $\mu\text{m}$ , Si is an excellent high-index material, while  $\text{SiO}_2$  and  $\text{Al}_2\text{O}_3$  are used as low-index counterparts and are transparent until 7  $\mu\text{m}$  [87]. The large electronic band gaps of  $\text{Nb}_2\text{O}_5$  and  $\text{SiO}_2$ —4 and 7.5 eV, respectively—allow for the avoidance of nonlinear effects in the infrared range, permitting development and production of

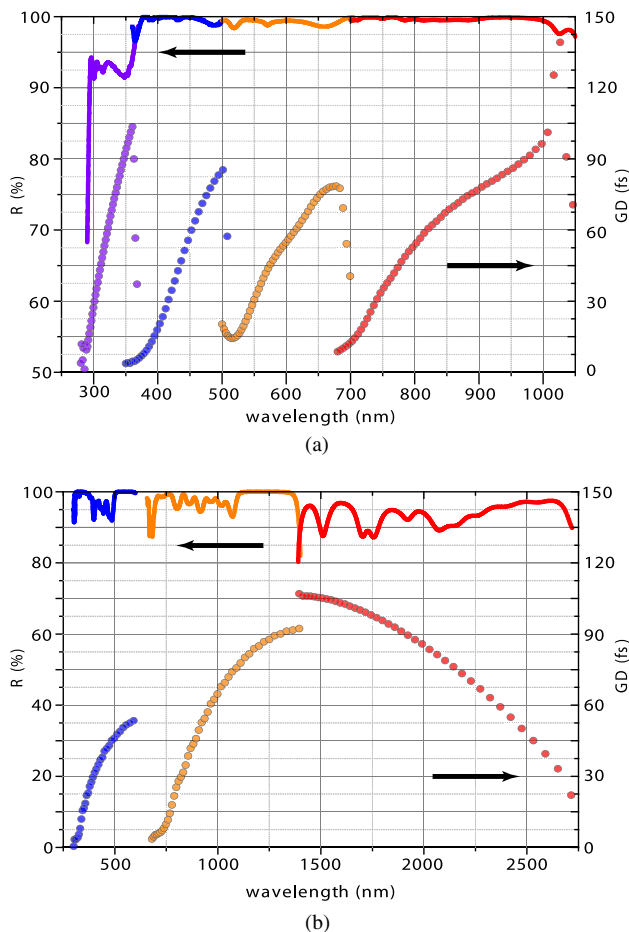


**Fig. 8.** Dispersive multilayers spanning over three optical octaves developed and produced for OWS. (a) Chirped mirrors developed and produced for the passive OWS in [43,91]. (b) Chirped mirrors under development and production for the passive and active infrared OWSs. Solid curves, designed reflectance; dotted curves, designed GD.

a broad class of efficient, precise, and flexible multilayer designs essential for broadband pulse manipulation.

## 6. CONCLUSIONS

Over the last two decades, dispersive multilayer optics have become standard components of ultrashort pulse laser systems and have defined the frontiers of ultrafast technology. In cooperation with well-controlled optical nonlinearities they permitted, for the first time, the generation of near-bandwidth-limited, near-single-cycle optical pulses. These in turn opened the door (by yet another nonlinear process: high-order harmonic generation) to the production of isolated attosecond extreme ultraviolet (XUV) pulses, the dispersion control of which also benefits from aperiodic multilayer structures [88–90].

Next-generation attosecond metrology calls for versatile control of the electromagnetic force of light within a half cycle of its oscillation. This calls for multi-octave superposition of optical fields with adjustable phase and amplitude—OWS in brief. Again, aperiodic dielectric multilayers constitute an enabling technology for this latest frontier of ultrafast science.

Figure 8(a) summarizes the dispersive mirrors controlling few-cycle pulses in the four channels of a two-octave-spanning

UV-VIS-NIR synthesizer, which has recently been demonstrated to be capable of generating a wide range of sub-cycle to few-cycle light transients, including sub-femtosecond optical pulses for the first time [43]. Figure 8(b), in turn, depicts dispersive mirrors developed for a prototypical three-channel device covering the entire near IR and reaching out into the mid IR, which is currently under construction.

State-of-the-art multilayer deposition technology had to rise to several challenges to be able to produce dispersive mirrors with the required precision in previously inaccessible wavelength ranges. Extension of the dispersive multilayer technology into the UV spectral range required both improved precision in depositing the nanometer-thick layers and new design paradigms to avoid undesirable nonlinear effects coming into play. On the other hand, pushing the opposite spectral frontier of dispersive multilayer optics to ever-longer wavelengths calls for new parameter optimization of coating algorithms for providing an optimal balance between the best possible mechanical and optical properties of ever-broader multilayer structures.

At present, precision dispersive multilayer designs span the working range of three octaves, allowing for precise and efficient dispersion control of light waveforms composed of signals all the way from ultraviolet (0.29  $\mu\text{m}$ ) to mid-infrared (2.7  $\mu\text{m}$ ) wavelengths. They define the cutting edge of ultrafast technology and pave the way toward new research directions based on dramatic advances in our capability to control atomic-scale electronic motions. In spite of all these advances, the technology is far from approaching its ultimate limits. Ongoing persistent technological efforts, driven by a range of scientific applications, are likely to expand the frontiers of multilayer-based optical dispersion control by several more octaves in the years to come.

**Funding.** Army Research Office (ARO) (W911NF-15-1-0360); Max-Planck-Gesellschaft (MPG); Munich-Centre for Advanced Photonics (MAP); Deutsche Forschungsgemeinschaft (DFG).

**Acknowledgment.** The authors thank Dr. M. Trubetskov for his continuous and invaluable contribution to the field; Drs. M. Th. Hassan, T.T. Luu, and E. Goulielmakis for fruitful discussions that yielded development of the dispersive designs in Fig. 1(a) and Fig. 8(a); Dr. A. Sommer for discussions that resulted in the designs of Fig. 3; and Dr. N. Karpowicz for the ideas of Fig. 7. We are also grateful to Dr. M. Weidman for his assistance with the styling of the text.

## REFERENCES

1. T. H. Maiman, "Stimulated optical radiation in ruby," *Nature* **187**, 493–494 (1960).
2. A. J. DeMaria, "Self mode-locking of lasers with saturable absorbers," *Appl. Phys. Lett.* **8**, 174–176 (1966).
3. E. Ippen, "Passive mode locking of the cw dye laser," *Appl. Phys. Lett.* **21**, 348–350 (1972).
4. R. L. Fork, "Generation of optical pulses shorter than 0.1 psec by colliding pulse mode locking," *Appl. Phys. Lett.* **38**, 671–673 (1981).
5. J. A. Valdmanis, R. L. Fork, and J. P. Gordon, "Generation of optical pulses as short as 27 femtoseconds directly from a laser balancing self-phase modulation, group-velocity dispersion, saturable absorption, and saturable gain," *Opt. Lett.* **10**, 131–133 (1985).
6. D. E. Spence, P. N. Kean, and W. Sibbett, "60-fsec pulse generation from a self-mode-locked Ti:sapphire laser," *Opt. Lett.* **16**, 42–44 (1991).



7. C.-P. Huang, H. Nathel, M. T. Asaki, S. Backus, M. M. Murnane, and H. C. Kapteyn, "17-fs pulses from a self-mode-locked Ti:sapphire laser," *Opt. Lett.* **17**, 1289–1291 (1992).
8. M. T. Asaki, C.-P. Huang, D. Garvey, J. Zhou, H. C. Kapteyn, and M. M. Murnane, "Generation of 11-fs pulses from a self-mode-locked Ti:sapphire laser," *Opt. Lett.* **18**, 977–979 (1993).
9. J. Zhou, I. P. Christov, G. Taft, C.-P. Huang, M. M. Murnane, and H. C. Kapteyn, "Pulse evolution in a broad-bandwidth Ti:sapphire laser," *Opt. Lett.* **19**, 1149–1151 (1994).
10. E. Treacy, "Optical pulse compression with diffraction gratings," *IEEE J. Quantum Electron.* **5**, 454–458 (1969).
11. R. Szipöcs, C. Spielmann, F. Krausz, and K. Ferencz, "Chirped multilayer coatings for broadband dispersion control in femtosecond lasers," *Opt. Lett.* **19**, 201–203 (1994).
12. A. Stingl, R. Szipöcs, C. Spielmann, and F. Krausz, "Generation of 11-fs pulses from a Ti:sapphire laser without the use of prisms," *Opt. Lett.* **19**, 204–206 (1994).
13. A. Stingl, R. Szipöcs, M. Lenzner, C. Spielmann, and F. Krausz, "Sub-10-fs mirror-dispersion-controlled Ti:sapphire laser," *Opt. Lett.* **20**, 602–604 (1995).
14. C. Spielmann, P. F. Curley, T. Brabec, and F. Krausz, "Ultrabroadband femtosecond lasers," *IEEE J. Quantum Electron.* **30**, 1100–1114 (1994).
15. R. Fluck, I. D. Jung, G. Zhang, F. X. Kärtner, and U. Keller, "Broadband saturable absorber for 10-fs pulse generation," *Opt. Lett.* **21**, 743–745 (1996).
16. I. D. Jung, F. X. Kärtner, N. Matuschek, D. H. Sutter, F. Morier-Genoud, G. Zhang, U. Keller, V. Scheuer, M. Tilsch, and T. Tschudi, "Self-starting 6.5-fs pulses from a Ti:sapphire laser," *Opt. Lett.* **22**, 1009–1011 (1997).
17. U. Morgner, F. X. Kärtner, S.-H. Cho, Y. Chen, H. A. Haus, J. G. Fujimoto, E. P. Ippen, V. Scheuer, G. Angelow, and T. Tschudi, "Sub-two-cycle pulses from a Kerr-lens mode-locked Ti:sapphire laser," *Opt. Lett.* **24**, 411–413 (1999).
18. D. H. Sutter, G. Steinmeyer, L. Gallmann, N. Matuschek, F. Morier-Genoud, U. Keller, V. Scheuer, G. Angelow, and T. Tschudi, "Semiconductor saturable-absorber mirror-assisted Kerr-lens mode-locked Ti:sapphire laser producing pulses in the two-cycle regime," *Opt. Lett.* **24**, 631–633 (1999).
19. R. Ell, U. Morgner, F. X. Kärtner, J. G. Fujimoto, E. P. Ippen, V. Scheuer, G. Angelow, T. Tschudi, M. J. Lederer, A. Boiko, and B. Luther-Davies, "Generation of 5-fs pulses and octave-spanning spectra directly from a Ti:sapphire laser," *Opt. Lett.* **26**, 373–375 (2001).
20. M. Nisoli, S. De Silvestri, G. Valiulis, and A. Varanavicius, "Fivefold femtosecond pulse compression by sum frequency generation," *Appl. Phys. Lett.* **68**, 3540–3542 (1996).
21. M. Nisoli, S. De Silvestri, and O. Svelto, "Generation of high energy 10 fs pulses by a new pulse compression technique," *Appl. Phys. Lett.* **68**, 2793–2795 (1996).
22. F. Théberge, N. Aközbek, W. Liu, A. Becker, and S. L. Chin, "Tunable ultrashort laser pulses generated through filamentation in gases," *Phys. Rev. Lett.* **97**, 023904 (2006).
23. T. Fuji and T. Suzuki, "Generation of sub-two-cycle mid-infrared pulses by four-wave mixing through filamentation in air," *Opt. Lett.* **32**, 3330–3332 (2007).
24. S. A. Trushin, K. Kosma, W. Fub, and W. E. Schmid, "Sub-10-fs super-continuum radiation generated by filamentation of few-cycle 800 nm pulses in argon," *Opt. Lett.* **32**, 2432–2434 (2007).
25. A. M. Weiner, "Femtosecond pulse shaping using spatial light modulators," *Rev. Sci. Instrum.* **71**, 1929–1960 (2000).
26. A. M. Weiner, D. E. Leaird, J. S. Patel, and J. R. Wullert, "Programmable femtosecond pulse shaping by use of a multielement liquid-crystal phase modulator," *Opt. Lett.* **15**, 326–328 (1990).
27. E. Matsubara, K. Yamane, T. Sekikawa, and M. Yamashita, "Generation of 2.6 fs optical pulses using induced-phase modulation in a gas-filled hollow fiber," *J. Opt. Soc. Am. B* **24**, 985–989 (2007).
28. E. Zeek, K. Maginnis, S. Backus, U. Russek, M. Murnane, G. Mourou, H. Kapteyn, and G. Vdovin, "Pulse compression by use of deformable mirrors," *Opt. Lett.* **24**, 493–495 (1999).
29. P. Tournois, "Acousto-optic programmable dispersive filter for adaptive compensation of group delay time dispersion in laser systems," *Opt. Commun.* **140**, 245–249 (1997).
30. F. Verluise, V. Laude, Z. Cheng, C. Spielmann, and P. Tournois, "Amplitude and phase control of ultrashort pulses by use of an acousto-optic programmable dispersive filter: pulse compression and shaping," *Opt. Lett.* **25**, 575–577 (2000).
31. V. Pervak, "Recent development and new ideas in the field of dispersive multilayer optics," *Appl. Opt.* **50**, C55–C61 (2011).
32. A. Verhoef, J. Seres, K. Schmid, Y. Nomura, G. Tempea, L. Veisz, and F. Krausz, "Compression of the pulses of a Ti:sapphire laser system to 5 femtoseconds at 0.2 terawatt level," *Appl. Phys. B* **82**, 513–517 (2006).
33. W. Schweinberger, A. Sommer, E. Bothschafter, J. Li, F. Krausz, R. Kienberger, and M. Schultze, "Waveform-controlled near-single-cycle milli-joule laser pulses generate sub-10 nm extreme ultraviolet continua," *Opt. Lett.* **37**, 3573–3575 (2012).
34. P. Paul, E. Toma, P. Breger, G. Mullot, F. Auge, P. Balcou, H. Muller, and P. Agostini, "Observation of a train of attosecond pulses from high harmonic generation," *Science* **292**, 1689–1692 (2001).
35. M. Hentschel, R. Kienberger, C. Spielmann, G. A. Reider, N. Milosevic, T. Brabec, P. Corkum, U. Heinzmann, M. Drescher, and F. Krausz, "Attosecond metrology," *Nature* **414**, 509–513 (2001).
36. G. Sansone, E. Benedetti, F. Calegari, C. Vozzi, L. Avaldi, R. Flammini, L. Poletto, P. Villoresi, C. Altucci, R. Velotta, S. Stagira, S. De Silvestri, and M. Nisoli, "Isolated single-cycle attosecond pulses," *Science* **314**, 443–446 (2006).
37. A. Baltuska, T. Udem, M. Uiberacker, M. Hentschel, E. Goulielmakis, C. Gohle, R. Holzwarth, V. S. Yakovlev, A. Scrinzi, T. Haensch, and F. Krausz, "Attosecond control of electronic processes by intense light fields," *Nature* **421**, 611–615 (2003).
38. E. Goulielmakis, M. Schultze, M. Hofstetter, V. S. Yakovlev, J. Gagnon, M. Uiberacker, A. L. Aquila, E. M. Gullikson, D. T. Attwood, R. Kienberger, F. Krausz, and U. Kleineberg, "Single-cycle nonlinear optics," *Science* **320**, 1614–1617 (2008).
39. S. E. Harris and A. V. Sokolov, "Subfemtosecond pulse generation by molecular modulation," *Phys. Rev. Lett.* **81**, 2894–2897 (1998).
40. R. K. Shelton, L.-S. Ma, H. C. Kapteyn, M. M. Murnane, J. L. Hall, and J. Ye, "Phase-coherent optical pulse synthesis from separate femtosecond lasers," *Science* **293**, 1286–1289 (2001).
41. G. Krauss, S. Lohss, T. Hanke, A. Sell, S. Eggert, R. Huber, and A. Leitenstorfer, "Synthesis of a single cycle of light with compact erbium-doped fibre technology," *Nat. Photonics* **4**, 33–36 (2010).
42. A. Wirth, M. T. Hassan, I. Grguras, J. Gagnon, A. Moulet, T. T. Luu, S. Pabst, R. Santra, Z. A. Alahmed, A. M. Azzeer, V. S. Yakovlev, V. Pervak, F. Krausz, and E. Goulielmakis, "Synthesized light transients," *Science* **334**, 195–200 (2011).
43. M. T. Hassan, T. T. Luu, A. Moulet, O. Raskazovskaya, P. Zhokhov, M. Garg, N. Karpowicz, A. M. Zheltikov, V. Pervak, F. Krausz, and E. Goulielmakis, "Optical attosecond pulses and tracking the nonlinear response of bound electrons," *Nature* **530**, 66–70 (2016).
44. S.-W. Huang, G. Cirmi, J. Moses, K.-H. Hong, S. Bhardwaj, J. R. Birge, L.-J. Chen, E. Li, B. J. Eggleton, G. Cerullo, and F. X. Kärtner, "High-energy pulse synthesis with sub-cycle waveform control for strong-field physics," *Nat. Photonics* **5**, 475–479 (2011).
45. S.-W. Huang, G. Cirmi, J. Moses, K.-H. Hong, S. Bhardwaj, J. R. Birge, L.-J. Chen, I. V. Kabakova, E. Li, B. J. Eggleton, G. Cerullo, and F. X. Kärtner, "Optical waveform synthesizer and its application to high-harmonic generation," *J. Phys. B* **45**, 074009 (2012).
46. H. Fattahi, H. G. Barros, M. Gorjan, T. Nubbemeyer, B. Alsaif, C. Y. Teisset, M. Schultze, S. Prinz, M. Haefner, M. Ueffing, A. Alismail, L. Vámos, A. Schwarz, O. Pronin, J. Brons, X. T. Geng, G. Arisholm, M. Ciappina, V. S. Yakovlev, D.-E. Kim, A. M. Azzeer, N. Karpowicz, D. Sutter, Z. Major, T. Metzger, and F. Krausz, "Third-generation femtosecond technology," *Optica* **1**, 45 (2014).
47. C. Manzoni, O. D. Mücke, G. Cirmi, S. Fang, J. Moses, S.-W. Huang, K.-H. Hong, G. Cerullo, and F. X. Kärtner, "Coherent pulse synthesis: towards sub-cycle optical waveforms," *Laser Photon. Rev.* **9**, 129–171 (2015).
48. O. D. Mücke, S. Fang, G. Cirmi, G. M. Rossi, S.-H. Chia, H. Ye, Y. Yang, R. Mainz, C. Manzoni, P. Farinello, G. Cerullo, and F. X. Kärtner, "Toward waveform nonlinear optics using multimillijoule sub-cycle waveform synthesizers," *IEEE J. Sel. Top. Quantum Electron.* **21**, 1–12 (2015).
49. V. Pervak, O. Raskazovskaya, I. B. Angelov, K. L. Vodopyanov, and M. Trubetskov, "Dispersive mirror technology for ultrafast lasers in the range 220–4500 nm," *Adv. Opt. Technol.* **3**, 55–63 (2014).

50. S.-H. Chia, G. Cirmi, S. Fang, G. M. Rossi, O. D. Mücke, and F. X. Kärtner, "Two-octave-spanning dispersion-controlled precision optics for sub-optical-cycle waveform synthesizers," *Optica* **1**, 315–333 (2014).
51. G. Tempea, F. Krausz, C. Spielmann, and K. Ferencz, "Dispersion control over 150 THz with chirped dielectric mirrors," *IEEE J. Sel. Top. Quantum Electron.* **4**, 193–196 (1998).
52. R. Szipöcs, "Dispersive properties of dielectric laser mirrors and their use in femtosecond pulse lasers," Ph.D. dissertation (University of Szeged, 2000).
53. N. Matuschek, L. Gallmann, D. Sutter, G. Steinmeyer, and U. Keller, "Back-side-coated chirped mirrors with ultra-smooth broadband dispersion characteristics," *Appl. Phys. B* **71**, 509–522 (2000).
54. G. Tempea, V. Yakovlev, B. Bacovic, F. Krausz, and K. Ferencz, "Tilted-front-interface chirped mirrors," *J. Opt. Soc. Am. B* **18**, 1747–1750 (2001).
55. M. Nisoli, S. De Silvestri, O. Svelto, R. Szipöcs, K. Ferencz, C. Spielmann, S. Sartania, and F. Krausz, "Compression of high-energy laser pulses below 5 fs," *Opt. Lett.* **22**, 522–524 (1997).
56. F. X. Kärtner, N. Matuschek, T. Schibli, U. Keller, H. A. Haus, C. Heine, R. Morf, V. Scheuer, M. Tilsch, and T. Tschudi, "Design and fabrication of double-chirped mirrors," *Opt. Lett.* **22**, 831–833 (1997).
57. N. Matuschek, F. X. Kärtner, and U. Keller, "Analytical design of double-chirped mirrors with custom-tailored dispersion characteristics," *IEEE J. Quantum Electron.* **35**, 129–137 (1999).
58. N. Matuschek, F. X. Kärtner, and U. Keller, "Theory of double-chirped mirrors," *IEEE J. Sel. Top. Quantum Electron.* **4**, 197–208 (1998).
59. F. X. Kärtner, U. Morgner, R. Ell, T. Schibli, J. G. Fujimoto, E. P. Ippen, V. Scheuer, G. Angelow, and T. Tschudi, "Ultrabroadband double-chirped mirror pairs for generation of octave spectra," *J. Opt. Soc. Am. B* **18**, 882–885 (2001).
60. V. Pervak, I. Ahmad, M. K. Trubetskov, A. V. Tikhonravov, and F. Krausz, "Double-angle multilayer mirrors with smooth dispersion characteristics," *Opt. Express* **17**, 7943–7951 (2009).
61. A. V. Tikhonravov, M. K. Trubetskov, and G. W. DeBell, "Application of the needle optimization technique to the design of optical coatings," *Appl. Opt.* **35**, 5493–5508 (1996).
62. A. V. Tikhonravov, M. K. Trubetskov, and G. W. DeBell, "Optical coating design approaches based on the needle optimization technique," *Appl. Opt.* **46**, 704–710 (2007).
63. A. V. Tikhonravov and M. K. Trubetskov, "Modern design tools and a new paradigm in optical coating design," *Appl. Opt.* **51**, 7319–7332 (2012).
64. V. Pervak, A. Tikhonravov, M. Trubetskov, S. Naumov, F. Krausz, and A. Apolonski, "1.5-octave chirped mirror for pulse compression down to sub-3 fs," *Appl. Phys. B* **87**, 5–12 (2007).
65. R. Trebino, K. W. DeLong, D. N. Fittinghoff, J. N. Sweetser, M. A. Krumbügel, B. A. Richman, and D. J. Kane, "Measuring ultrashort laser pulses in the time-frequency domain using frequency-resolved optical gating," *Rev. Sci. Instrum.* **68**, 3277–3295 (1997).
66. C. Iaconis and I. Walmsley, "Spectral phase interferometry for direct electric-field reconstruction of ultrashort optical pulses," *Opt. Lett.* **23**, 792–794 (1998).
67. S. Keiber, S. Sederberg, A. Schwarz, M. Trubetskov, V. Pervak, F. Krausz, and N. Karpowicz, "Electro-optic sampling of near-infrared waveforms," *Nat. Photonics* **10**, 159–162 (2016).
68. M. Rhodes, G. Steinmeyer, and R. Trebino, "Standards for ultrashort-laser-pulse-measurement techniques and their consideration for self-referenced spectral interferometry," *Appl. Opt.* **53**, D1–D11 (2014).
69. M. N. Polyanskiy, "Refractive index database," <http://refractiveindex.info>.
70. C. A. Rivera, S. E. Bradforth, and G. Tempea, "Gires-Tournois interferometer type negative dispersion mirrors for deep ultraviolet pulse compression," *Opt. Express* **18**, 18615–18624 (2010).
71. V. Pervak, F. Krausz, and A. Apolonski, "Hafnium oxide thin films deposited by reactive middle-frequency dual-magnetron sputtering," *Thin Solid Films* **515**, 7984–7989 (2007).
72. R. DeSalvo, A. A. Said, D. J. Hagan, E. W. Van Stryland, and M. Sheik-Bahae, "Infrared to ultraviolet measurements of two-photon absorption and  $n$  2 in wide bandgap solids," *IEEE J. Quantum Electron.* **32**, 1324–1333 (1996).
73. O. Razskazovskaya, T. T. Luu, M. Trubetskov, E. Goulielmakis, and V. Pervak, "Nonlinear absorbance in dielectric multilayers," *Optica* **2**, 803–811 (2015).
74. E. Fedulova, M. Trubetskov, T. Amotchkina, K. Fritsch, P. Baum, O. Pronin, and V. Pervak, "Kerr effect in multilayer dielectric coatings," *Opt. Express* **24**, 21802–21817 (2016).
75. O. Razskazovskaya, M. T. Hassan, T. Luu, E. Goulielmakis, and V. Pervak, "Efficient broadband highly dispersive  $\text{HfO}_2/\text{SiO}_2$  multilayer mirror for pulse compression in near ultraviolet," *Opt. Express* **24**, 13628–13633 (2016).
76. P. G. Antal and R. Szipöcs, "Relationships among group delay, energy storage, and loss in dispersive dielectric mirrors," *Chin. Opt. Lett.* **10**, 053101 (2012).
77. I. B. Angelov, M. von Pechmann, M. K. Trubetskov, F. Krausz, and V. Pervak, "Optical breakdown of multilayer thin-films induced by ultra-short pulses at MHz repetition rates," *Opt. Express* **21**, 31453–31461 (2013).
78. F. Krausz and M. I. Stockman, "Attosecond metrology: from electron capture to future signal processing," *Nat. Photonics* **8**, 205–213 (2014).
79. A. Gordon and F. X. Kärtner, "Scaling of keV HHG photon yield with drive wavelength," *Opt. Express* **13**, 2941–2947 (2005).
80. T. Popmintchev, M.-C. Chen, P. Arpin, M. M. Murnane, and H. C. Kapteyn, "The attosecond nonlinear optics of bright coherent X-ray generation," *Nat. Photonics* **4**, 822–832 (2010).
81. T. Popmintchev, M.-C. Chen, D. Popmintchev, P. Arpin, S. Brown, S. Alisauskas, G. Andriukaitis, T. Balciunas, O. D. Mücke, A. Pugzlys, A. Baltuska, B. Shim, S. E. Schrauth, A. Gaeta, C. Hernandez-Garcia, L. Plaja, A. Becker, A. Jaron-Becker, M. M. Murnane, and H. C. Kapteyn, "Bright coherent ultrahigh harmonics in the keV X-ray regime from mid-infrared femtosecond lasers," *Science* **336**, 1287–1291 (2012).
82. C. Vozzi, G. Cirmi, C. Manzoni, E. Benedetti, F. Calegari, G. Sansone, S. De Silvestri, M. Nisoli, and G. Cerullo, "High-energy, few-optical-cycle pulses at 1.5  $\mu\text{m}$  with passive carrier-envelope phase stabilization," *Opt. Express* **14**, 10109–10116 (2006).
83. X. Gu, G. Marcus, Y. Deng, T. Metzger, C. Teisset, N. Ishii, T. Fuji, A. Baltuska, R. Butkus, V. Pervak, H. Ishizuki, T. Taira, T. Kobayashi, R. Kienberger, and F. Krausz, "Generation of carrier-envelope-phase-stable 2-cycle 740-J pulses at 2.1- $\mu\text{m}$  carrier wavelength," *Opt. Express* **17**, 62–69 (2009).
84. G. Andriukaitis, T. Balciunas, S. Ališauskas, A. Pugzlys, A. Baltuska, T. Popmintchev, M.-C. Chen, M. M. Murnane, and H. C. Kapteyn, "90 GW peak power few-cycle mid-infrared pulses from an optical parametric amplifier," *Opt. Lett.* **36**, 2755–2757 (2011).
85. N. Demirdöven, M. Khalil, O. Golonzka, and A. Tokmakoff, "Dispersion compensation with optical materials for compression of intense sub-100-fs mid-infrared pulses," *Opt. Lett.* **27**, 433–435 (2002).
86. J. A. Gruetzmacher and N. F. Scherer, "Few-cycle mid-infrared pulse generation, characterization, and coherent propagation in optically dense media," *Rev. Sci. Instrum.* **73**, 2227–2236 (2002).
87. M. Friz and F. Waibel, "Coating materials," in *Optical Interference Coatings* (Springer, 2003), pp. 105–130.
88. C. Bourassin-Bouchet, S. De Rossi, J. Wang, E. Meltchakov, A. Giglia, N. Mahne, S. Nannarone, and F. Delmotte, "Shaping of single-cycle sub-50-attosecond pulses with multilayer mirrors," *New J. Phys.* **14**, 023040 (2012).
89. M. Hofstetter, M. Schultze, M. Fiess, B. Dennhardt, A. Guggenmos, J. Gagnon, V. S. Yakovlev, E. Goulielmakis, R. Kienberger, E. M. Gullikson, F. Krausz, and U. Kleineberg, "Attosecond dispersion control by extreme ultraviolet multilayer mirrors," *Opt. Express* **19**, 1767–1776 (2011).
90. A. Guggenmos, M. Hofstetter, R. Rauhut, B. Nickel, E. Gullikson, and U. Kleineberg, "Aperiodic multilayer mirrors for attosecond soft x-ray pulses," *Proc. SPIE* **8502**, 850204 (2012).
91. M. T. Hassan, A. Wirth, I. Grgura, A. Moulet, T. T. Luu, J. Gagnon, V. Pervak, and E. Goulielmakis, "Invited article: attosecond photonics: synthesis and control of light transients," *Rev. Sci. Instrum.* **83**, 111301 (2012).